# DECOUPLING LAYOUT FROM GLYPH IN ONLINE CHINESE HANDWRITING GENERATION

**Anonymous authors**
Paper under double-blind review

## ABSTRACT

Text plays a crucial role in the transmission of human civilization, and teaching machines to generate online handwritten text in various styles presents an interesting and significant challenge. However, most prior work has concentrated on generating individual Chinese fonts, leaving *complete text line generation largely unexplored*. In this paper, we identify that text lines can naturally be divided into two components: layout and glyphs. Based on this division, we designed a text line layout generator coupled with a diffusion-based stylized font synthesizer to address this challenge hierarchically. More concretely, the layout generator performs in-context-like learning based on the text content and the provided style references to generate positions for each glyph autoregressively. Meanwhile, the font synthesizer which consists of a character embedding dictionary, a multi-scale calligraphy style encoder and a 1D U-Net based diffusion denoiser will generate each font on its position while imitating the calligraphy style extracted from the given style references. Qualitative and quantitative experiments on the CASIA-OLHWDB demonstrate that our method is capable of generating structurally correct and indistinguishable imitation samples.

## 1 INTRODUCTION

Deep generative models, such as GANs (Goodfellow et al., 2014), VAEs (Kingma & Welling, 2014), and diffusion models (Sohl-Dickstein et al., 2015; Ho et al., 2021), have demonstrated a formidable ability to generate a wide array of data types. Handwritten data, which encompasses language characters, mathematical symbols, sketches, and diagrams, represents a highly personalized form of data with a wide range of application scenarios. Creating handwriting can provide personalized writing service or be used for data augmentation for document analysis models (Lai et al., 2021; Kang et al., 2021; Xie et al., 2020). In recent years, the emergence of extensive datasets has prompted a notable surge in the application of generative modeling techniques to handwritten data (Xu et al., 2022; Aksan et al., 2018).

Among handwritten data, the generation of Chinese handwritten texts has garnered increasing attention due to their widespread use and the greater challenges they present compared to Latin scripts (Gao et al., 2019; Liu et al., 2022). A crucial aspect of this task is ensuring the integrity and accuracy of the structural composition of the characters. The vast diversity and complex geometric structures of these characters render this task particularly challenging. Another important consideration is how to imitate specific personal writing styles while maintaining structural correctness (Yang et al., 2024; Gan & Wang, 2021; Xie et al., 2021; Kong et al., 2022). Compared to individual characters, text lines serve as more effective communication tools, capable of conveying more complex information and emotions. However, the majority of prior research has primarily focused on generating individual Chinese fonts, largely overlooking the significantly more challenging task of generating complete text lines.

In this work, we aim to *generate **stylized** and **coherent** online Chinese handwritten text lines based on specified text contents and given style reference samples*. A handwritten line of text can be viewed as composed of individual characters and their arrangement. Based on this observation, we propose a hierarchical method that disentangles the layout generation from the writing of individual characters during the generation of full lines. We design a novel text line layout generator to arrange positions for each character based on their categories and given handwriting style references. For

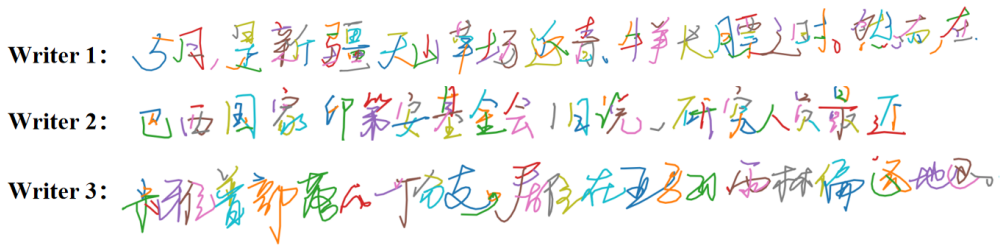


Figure 1: Handwritten text lines with vastly different styles generated by our methods. It is worth mentioning that the generated online data contains dynamic trajectory information, rather than just static images, enabling more interactive applications. Different colors represent different strokes, showcasing the dynamic process of writing.

font generation, we construct a 1D convolutional U-Net (Ronneberger et al., 2015) network and design a multi-scale feature fusion module to fully mimic the calligraphy characteristics of the given reference sample. We utilize the publicly available CASIA-OLHWDB dataset (Liu et al., 2011) for training and evaluating our method, showcasing its effectiveness through a combination of quantitative and qualitative experiments. Figure 1 shows several visualizations of our generated samples.

Our contributions can be summarized as: 1) We propose a hierarchical approach to solve the unexplored online handwritten Chinese text line generation task. 2) We introduce a simple but effective layout generator that can generate character positions based on the text contents and writing style through in-context-like learning. 3) We construct a 1D U-Net network for font generation and design a multi-scale contrastive-learning-based style encoder to improve the ability of calligraphy style imitation.

## 2 Related Work

### 2.1 Online Handwritten Data Generation

The most commonly adopted method (Graves, 2013) for generating online handwritten data involves combining neural network models for sequence data processing with a mixture of Gaussian distributions to model the movement information of the pen. Following this work, SketchRNN (Ha & Eck, 2018) adopts RNN as the encoder and decoder of VAE, conducting the task of unconditional sequence data generation. COSE (Aksan et al., 2020) treats drawings as a collection of strokes and projects variable-length strokes into a latent space of fixed dimension and uses MLPs to generate one single stroke based on its latent encoding autoregressively. Subsequently, there has been a growing emphasis in academic research on conditional generation, such as producing handwriting with specific contents or diverse writing styles (Aksan et al., 2018; Kotani et al., 2020; Tolosana et al., 2021). They extract calligraphic styles from reference samples and combine them with specific textual content to achieve controllable style English handwriting synthesis.

In contrast to alphabetic languages, Chinese encompasses a significantly larger character set and Chinese characters exhibit more intricate shapes and topological structures (Xu et al., 2009; Lin et al., 2015; Lian et al., 2018; Radford et al., 2016; Zhu et al., 2017). For this reason, *most methods designed for handwritten English generation do not work well when applied directly to Chinese*.

As for the field of online Chinese character generation, both LSTM and GRU models are employed simultaneously in (Zhang et al., 2017) to successfully generate readable Chinese characters of specific classes at the first time. FontRNN (Tang et al., 2019) focuses on stylized font generation, which utilizes a transfer-learning strategy to generate stylized Chinese characters. However, each trained model can only synthesize the same style as the train set. By adding a style encoder branch to the generator, DeepImitator (Zhao et al., 2020) can generate characters of any style given a few reference samples. They utilize a CNN as the calligraphy style encoder to extract style codes from offline images and a GRU as the generator to synthesize the online trajectories. Similarly, WriteLikeU (Tang & Lian, 2021), DiffWriter (Ren et al., 2023), and SDT (Dai et al., 2023) are also capable of handling this functionality.

### 2.2 Diffusion Model for Sequence Data

Diffusion model, first proposed in (Sohl-Dickstein et al., 2015) exhibits a remarkably robust capability in learning the data distribution and generating impressively high quality and diverse images in recent years (Luo, 2022; Ho et al., 2021; Dhariwal & Nichol, 2021; Song et al., 2020; Rombach et al., 2021). In terms of sequence data generation, NaturalSpeech2 (Shen et al., 2024) employs the latent diffusion framework to synthesize speech content with specific contents by imitating various tones and speaking styles. CHIRODIFF (Das et al., 2023) first utilizes diffusion for unconditional chirographic data generation and later DiffWriter (Ren et al., 2023) adopts diffusion models for online Chinese characters generation. *However, previous methods only explored how to apply the diffusion process to online handwritten data, lacking fine control over writing details.*

## 3 Methods

### 3.1 Preliminary

**Online Handwritten Data.** In general, online handwriting is a kind of *time series data*, which is composed of a series of trajectory points. Each point ($[h, v, s] \in \mathbb{R}^3$) contains the *horizontal movement*, *vertical movement* and *the state information* of the pen. We use $s = 1$ to represent the pen touching state and $s = -1$ to represent the pen lifting state, making it convenient to distinguish the two states by simply adopting dichotomy with threshold 0 after the addition of zero-mean standard Gaussian noise to the data.

**Data Notation.** A handwritten font that consists of $n$ points can be represented as $\mathbf{x} \in \mathbb{R}^{n\times 3}$. Its corresponding category is represented as a one-hot vector $\mathbf{c} \in \mathbb{R}^K$, where $K$ is the number of character categories. A handwritten text line can be represented as $\mathbf{X} = [\mathbf{x}^1, \cdots, \mathbf{x}^m] \in \mathbb{R}^{N\times 3}$, where $\mathbf{x}^i \in \mathbb{R}^{n^i\times 3}$ denotes the $i$-th character, $m$ denotes the number of characters, and $N$ denotes the number of points with $N = \sum_{i=1}^{m} n^i$. Its text content can be represented as $\mathbf{C} = [\mathbf{c}^1, ..., \mathbf{c}^m] \in \mathbb{R}^{m\times K}$.

**Problem Statement.** Given the text line content $\mathbf{C}$ and style reference samples $\mathbf{X}_{ref}$ (preferably a coherent handwritten text line) from a given author, our objective is to generate handwritten text lines with the specified content while imitating the author's writing habits. The conditional probability can be written as $p(\mathbf{X}|\mathbf{C}, \mathbf{X}_{ref})$. Unlike English, Chinese has a large number of character categories, each with its specific stroke order and geometric structure. The combinations to form a text line are endless. Therefore, the **most critical challenge** in generating handwritten Chinese text lines lies in two aspects: *1) Ensuring the correctness of the structure of each character while maintaining consistency with the chosen writing style. 2) Arranging the relative positions of different characters, especially between Chinese characters and punctuation marks, to achieve a natural and fluent layout for the entire handwritten text line.*

### 3.2 Analysis and Overview

Directly modeling $p(\mathbf{X}|\mathbf{C}, \mathbf{X}_{ref})$ is overwhelmingly challenging since the positions of glyphs are unknown. In this work, we treat the text line layout as latent variables in the text line generation and instead model the joint distribution of the text line and its layout: $p(\mathbf{X}, \text{Layout}_X|\mathbf{C}, \mathbf{X}_{ref})$.

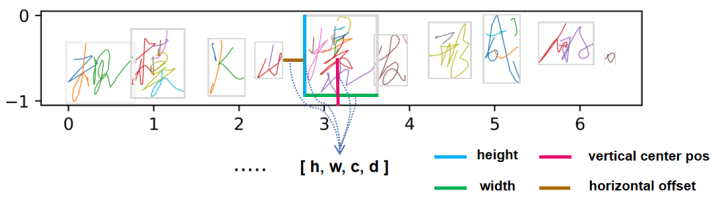


Figure 2: The illustration of character bounding box, consists of height, width, vertical center position and horizontal offset relative to the previous character.

In detail, we define the layout of a handwritten text line as the positions and sizes of all characters in the line. We calculate the `[height, width, vertical center position and horizontal offset relative to the previous character]` for each character as its bounding box, shown in Figure 2. In this way, the layout of $\mathbf{X}$ can be represented as: $\text{Layout}_X = [\text{Box}^1, \cdots, \text{Box}^m] \in \mathbb{R}^{m \times 4}$.

During the writing process, human beings typically take neighboring glyph positions into account for the current character position to ensure the continuity of the written text lines. However, when the positional information of each character is provided, the writing process of each character is relatively independent. Similarly, we assume that when the bounding box of a character is given, the generation of the character is independent of other characters. By this assumption, we can factorize $p(\mathbf{X}, \text{Layout}_X | \mathbf{C}, \mathbf{X}_{ref})$ as:

$$\begin{aligned} p(\mathbf{X}, \text{Layout}_X | \mathbf{C}, \mathbf{X}_{ref}) &= p(\text{Layout}_X | \mathbf{C}, \mathbf{X}_{ref}) p(\mathbf{X} | \mathbf{C}, \mathbf{X}_{ref}, \text{Layout}_X) \\ &= p(\text{Layout}_X | \mathbf{C}, \mathbf{X}_{ref}) \prod_{i=1}^{m} p(\mathbf{x}^i | \mathbf{c}^i, \mathbf{X}_{ref}, \text{Box}^i). \end{aligned} \tag{1}$$

Equation 1 inspires us to decouple the complete generation process into two components: **layout generation** $p(\text{Layout}_X | \mathbf{C}, \mathbf{X}_{ref})$ and **individual font synthesis** $p(\mathbf{x}^i | \mathbf{c}^i, \mathbf{X}_{ref}, \text{Box}^i)$. Correspondingly, our proposed model consists of two parts: *a text line layout generator* and *a stylized font synthesizer*, shown in Figure 3.

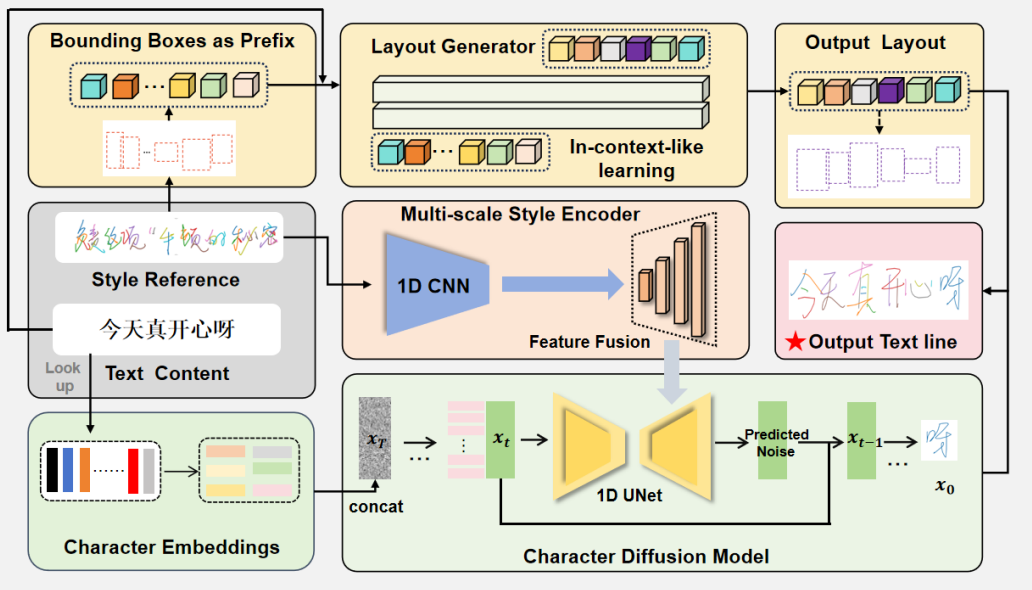


Figure 3: Overview of the proposed method, which consists of a layout generator and a font synthesizer. Given the text content and style references, the two modules operate simultaneously: the layout generator will arrange the bounding box of each character based on the overall style of the reference, while the font synthesizer will imitate the calligraphic style of the references to produce the corresponding handwritten fonts.

### 3.3 In-Context Layout Generator

**Modeling The Human Writing Process.** Considering the consistent and coherent style of the entire text layout when people write a complete text line, it is natural and reasonable to use a certain length of the prefix of the text line as context to predict the subsequent layout. Based on this observation, we decompose the generation of layout in an autoregressive manner:

$$p(\text{Layout}_X|\mathbf{C}, \mathbf{X}_{ref}) = p([\text{Box}^1, \cdots, \text{Box}^m]|\mathbf{C}, \mathbf{X}_{ref}) = \prod_{i=1}^{m} p(\text{Box}^i|[\text{Box}^1, \cdots, \text{Box}^{i-1}], \mathbf{c}^i, \mathbf{X}_{ref}), \tag{2}$$

which is akin to the human writing process. Denote the layout generator model as $\mathcal{G}$, which is an LSTM network in our work. The generation of the $i$-th character box can be represented as:

$$[\text{Box}^i, \mathbf{h}^i] = \mathcal{G}(\text{Box}^{i-1}, \mathbf{c}^i, \mathbf{h}^{i-1}), \tag{3}$$

where $\mathbf{h}$ represents the hidden state of LSTM. It is worth noting that *different glyphs, punctuation marks, and numbers generally have markedly different shapes*. Therefore, it is crucial to consider the character categories during the generation.

**Training Objective.** During the training phase, we employ the teacher-forcing technique and use the $\ell_1$ distance between ground truth and generated layout as the loss function. We empirically illustrate that this training method encourages the model to generate layouts that are consistent throughout the whole text line.

**In-Context Generation.** In order to mimic the layout style of the given reference sample, we *use the style reference samples as a prompt context*, inputting their true bounding boxes as a prefix instead of the generator $\mathcal{G}$'s outputs. The outputs corresponding to the prefix time steps are inconsequential, but the hidden state of the LSTM network implicitly contains information about the layout style. It will plan the subsequent layout according to the writing style of the prefix context.

We experimentally show that this approach effectively possesses the capability for in-context-like learning in this task, and therefore can imitate general writing styles unseen in the training set. Additionally, if no coherent text line is provided as the style reference sample, the model will perform unconditional layout planning with a prefix length of 0.

### 3.4 Stylized Diffusion Character Synthesizer

We adopt the conditional diffusion model as the generator for individual characters. However, previous diffusion-based methods for online handwritten data have neglected the multi-scale features of calligraphy style. To address this issue, we design a 1D U-Net network as the denoiser, and combine it with a character embedding dictionary and a multi-scale calligraphy style encoder to generate characters with specific categories and calligraphy styles.

#### 3.4.1 Model Architecture

**Character Embeddings.** Inspired by (Zhang et al., 2017), a dictionary is constructed to encode the structural information of characters: $\mathbf{E} \in \mathbb{R}^{K \times N_z}$, where $K$ represents the number of character categories and $N_z$ represents the code dimension. Each row in matrix E encodes the structure of one category. To generate a character of the $k$-th category, we first query the embedding dictionary and get the $k$-th row of matrix $\mathbf{E}[k] \in \mathbb{R}^{N_z}$ as the content code. Supposing the shape of noisy data $\mathbf{x}_t$ is $(n, 3)$, we duplicate the content code as well as sinusoidal position encoding of time $\text{emb}_t \in \mathbb{R}^{N_t}$ for $n$ times and concatenate them with the noisy data $\mathbf{x}_t$ to obtain the input $\mathbf{x}_{in} = [\mathbf{x}_t, \text{emb}_t, \mathbf{E}[k]] \in \mathbb{R}^{n \times (N_z + N_t + 3)}$ of the denoiser.

**Multi-Scale Style Encoder.** Compared to the global layout style, the calligraphy styles of individual characters are often reflected in various details, such as overall neatness, stroke length, and curvature. Considering that these characteristics are all at different scales, we construct a 1D convolutional style encoder that employs continuous downsampling layers to extract calligraphy features at different levels and a 1D U-Net denoiser to leverage these features.

**U-Net Denoiser.** The U-Net network *shares the same number of down-sampling layers and strides as the style encoder*. We set the number of down-sampling blocks as 3 in this work. This alignment ensures that during the decoding process, each layer's features in the U-Net can correspond to features of the same scale in the style encoder. These features are fused using the QKV cross-attention mechanism (Rombach et al., 2021), thereby incorporating multi-scale style information into the denoiser. The architectural diagram and further details can be found in Appendix B.2.2.

### 3.4.2 TRAINING OBJECTIVE

Denote the font synthesizer as $\mathcal{E}$, the loss function consists of two parts: a multi-scale style contrastive learning loss $\ell_c$ as well as a diffusion process reconstruction loss $\ell_r$:

$$\ell_{\mathcal{E}} = \ell_c + \ell_r. \tag{4}$$

We detail the two learning objectives as follows.

**Multi-Scale Style Contrastive Learning Loss.** To incentivize the style encoder to extract discriminative calligraphic style features from different authors across diverse scales, we perform contrastive learning on distinct feature layers respectively. More concretely, suppose a mini-batch $\{\mathbf{x}_{w_1}, \cdots, \mathbf{x}_{w_b}\}$ contains $b$ characters written by $b$ different authors $W = \{w_1, \cdots, w_b\}$ and let $A(w_i) = W \backslash \{w_i\}$. Recalling section 3.4.1, the style encoder SENC contains three downsampling blocks corresponding to three different scales of features for one character: $\text{SENC}(\mathbf{x}_{w_i}) = \{\boldsymbol{f}^1_{w_i}, \boldsymbol{f}^2_{w_i}, \boldsymbol{f}^3_{w_i}\}$.

For each scale features, take $\boldsymbol{f}^3_{w_i} \in \mathbb{R}^{L \times d}$ as an sample, where $L$ represents the length of the feature sequence and $d$ indicates the dimension of each feature vector. We randomly select two non-overlapping segments $\boldsymbol{e}^3_{w_i}, \boldsymbol{e}^{3+}_{w_i}$ from $\boldsymbol{f}^3_{w_i}$ ($\boldsymbol{e} \in \mathbb{R}^{l \times d}$ from the total length $L$), serving as a positive pair from author $w_i$. The contrastive loss for $f^3$ is formulated as:

$$\ell^3_c = -\frac{1}{n} \sum_{k=1}^{n} \log \frac{\exp\left(s(\boldsymbol{e}^3_{w_k}, \boldsymbol{e}^{3+}_{w_k})/\tau\right)}{\sum_{w_i \in A(w_k)} \exp\left(s(\boldsymbol{e}^3_{w_k}, \boldsymbol{e}^{3+}_{w_i})/\tau\right)}, \tag{5}$$

where $s(\boldsymbol{e}^3_{w_k}, \boldsymbol{e}^{3+}_{w_k}) = g^3(\boldsymbol{e}^3_{w_k})^T g^3(\boldsymbol{e}^{3+}_{w_k})$, $\tau$ is a temperature parameter, $g^3$ is a linear projection. Similarly, we can obtain $\ell^1_c$ and $\ell^2_c$. The overall multi-scale contrastive loss is formulated as:

$$\ell_c = \lambda_1 \ell^1_c + \lambda_2 \ell^2_c + \lambda_3 \ell^3_c, \tag{6}$$

where $\lambda_1, \lambda_2, \lambda_3$ are empirical weights. We set $\lambda_1 = 0.01, \lambda_2 = \lambda_3 = 0.1$ in this work.

**Diffusion Reconstruction Loss and Generation Process.** Given a target character $\mathbf{x}$ and style reference samples $\mathbf{X}_{ref}$ which is a piece of handwritten text line written by the same writer. Denoting the style encoder as SENC, and the character embedding dictionary as E, the diffusion reconstruction loss is calculated in Algorithm 1. $T, \{\alpha_t\}, \overline{\alpha}_t$ are hyperparameters of diffusion models, which are introduced in Appendix B.1. Correspondingly, given the character category $k$ and style reference samples $\mathbf{X}_{ref}$, we randomly sample standard Gaussian noise as $\mathbf{x}_T \in \mathbb{R}^{(n \times 3)}$, where $n$ is the max length, the generation procedure is summarized in Algorithm 2.

**Algorithm 1** Diffusion Reconstruction Loss $\ell_r$

**procedure** TRAIN( $\mathbf{x}$, $\mathbf{X}_{ref}$, $k$, $T$, $\{\alpha_t\}$)

  Sample $t \in (1, T)$, $\epsilon \in \mathcal{N}(0, 1)$
  $\mathbf{x}_t = \sqrt{\overline{\alpha}_t}\mathbf{x}_0 + \sqrt{1 - \overline{\alpha}_t}\epsilon$
  $\mathbf{x}_{in} = \text{concat}(\mathbf{x}_t, \text{emb}_t, \text{E}[k])$
  $f_{style} = \text{SENC}(\mathbf{X}_{ref})$
  $\epsilon_\theta = \mathcal{E}(\mathbf{x}_{in}, f_{style})$
  $\ell_r(\theta) = ||\epsilon - \epsilon_\theta||^2$
  **Output:** $\ell_r$

**end procedure**

**Algorithm 2** Font Generation Process

**procedure** GEN($\mathbf{x}_T$, $k$, $\mathbf{X}_{ref}$, $T$, $\{\alpha_t\}$)
  $f_{style} = \text{SENC}(\mathbf{X}_{ref})$
  **for** $t = T, T-1, ..., 1$ **do**
    $\mathbf{x}_{in} = \text{concat}(\mathbf{x}_t, \text{emb}_t, \text{E}[k])$
    $\epsilon_\theta = \mathcal{E}(\mathbf{x}_{in}, f_{style})$
    $\mu_\theta(\mathbf{x}_t) = \frac{1}{\sqrt{\alpha_t}}\mathbf{x}_t - \frac{1-\alpha_t}{\sqrt{1-\overline{\alpha}_t}\sqrt{\alpha_t}}\epsilon_\theta$
    $\sigma^2_t = \frac{(1-\alpha_t)(1-\overline{\alpha}_{t-1})}{1-\overline{\alpha}_t}$
    $\mathbf{x}_{t-1} = \mu_\theta(\mathbf{x}_t) + \sigma_t z, z \sim \mathcal{N}(0, I)$
  **end for**
  **Output:** $\mathbf{x}_0$
**end procedure**

## 4 EXPERIMENTS

In the experimental section, we assess our approach in three areas: **capability of calligraphy style imitation**, **capability of layout style imitation**, and **content readability**, utilizing both qualitative and quantitative experiments as followings:

### 4.1 DATASET

We use the CASIA Online Chinese Handwriting Databases (Liu et al., 2011) to train and test our model. For single character generation, following previous work, the CASIA-OLHWDB (1.0-1.2) is adopted as the training set, which contains about 3.7 million online Chinese handwritten characters produced by 1,020 writers. The ICDAR-2013 competition database (Yin et al., 2013b) is adopted as the test set, which contains 60 writers, with each contributing the 3,755 most frequently used characters set of GB2312-80. For layout and text line generation, we adopt CASIA-OLHWDB (2.0-2.2) which consists of approximately 52,000 text lines written by 1,200 authors, totaling 1.3 million characters. We take 1,000 writers as the training set and the left 200 writers as the test set. Detailed descriptions of data preprocessing, model architecture, and training process are provided in Appendix B.2.

### 4.2 FONT GENERATION

**Evaluation Metrics.** To assess the model's ability to imitate calligraphy style and generate accurate character structures, we adopt three core indicators DTW (Normalized Dynamic Time Warping Distance), Content Score, and Style Score following previous work (see Appendix B.2 for details). For each writing style in the test set, we randomly generate 100 characters, totaling 6,000 characters, to measure the performance.

**Baselines and Results.** There are mainly two types of online handwritten Chinese character generation approaches: the first type comprises purely data-driven methods that learn the structure of characters and calligraphy style only from the training set. The second type requires a standard printed font image as an auxiliary input, and train models to transform the standard fonts into characters with a specific writing style. The advantage of the second method is that it is easier to generate correct structures, but it cannot generate characters without corresponding standard glyphs and the computational cost will be heavier. As shown in Table 1, being a method of the first type, our model achieves state-of-the-art performance in all pure data-driven approaches and is comparable to state-of-the-art style transfer-based methods.

**Effects of Contrastive Learning.** In this experiment, we randomly select 5 writers in the test set, 150 characters for each writer. We first use the style encoder to extract their features and visualize them using the $t$-SNE method (Van der Maaten & Hinton, 2008). As shown in Figure 4, the right side was obtained through our fully trained style encoder, while the left side does not adopt contrastive learning loss. In the right figure, features from the same author usually exhibit a *clear clustering trend*, while in the left figure, the distribution is more *random and scattered*. It illustrates that through contrastive learning, the calligraphy style encoder can extract discriminative features effectively.

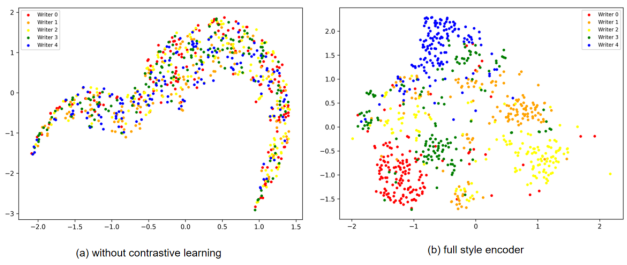


Figure 4: $t$-SNE visualization of the font style features. Different colors represent different writers.

Figure 5: The ablation of multi-scale contrastive learning.

| $\lambda_1$ | $\lambda_2$ | $\lambda_3$ | Style Score | Content Score |
|---|---|---|---|---|
| 0.0 | 0.0 | 0.0 | 0.875 | 0.893 |
| 0.0 | 0.0 | 0.1 | 0.900 | 0.887 |
| 0.01 | 0.1 | 0.1 | 0.918 | 0.891 |

**Different Weights for Contrastive Learning.** In Table 5, $\lambda_1, \lambda_2, \lambda_3$ are empirical weights in equation 6. A weight of 0 indicates that the loss is not used in this feature layer. We find that while the Content Score is basically unaffected, the Style Score experiences a certain improvement, particularly with the implementation of multi-scale contrastive learning.

Table 1: Evaluation of Character Structure Accuracy and Calligraphy Style Imitation.

| Methods | Purely data-driven | | | Style transfer | | |
|---|---|---|---|---|---|---|
| | DeepImitator | DiffWriter | **Ours** | FontRNN | WriteLikeU | SDT |
| DTW (↓) | 1.062 | 0.997 | **0.932** | 1.045 | 0.982 | 0.880 |
| Content Score (↑) | 0.834 | 0.887 | **0.891** | 0.875 | 0.938 | 0.970 |
| Style Score (↑) | 0.432 | 0.481 | **0.918** | 0.461 | 0.711 | 0.945 |

### 4.3 Full Line Generation

#### 4.3.1 Evaluation Metrics

**Layout Assessment.** The core of our method lies in the in-context layout generation. To better demonstrate the effectiveness of our method, we adopt several *binary geometric features* from traditional OCR (Zhou et al., 2007; Yin et al., 2013a) that can effectively reflect the characteristics of character spatial relations within text lines, shown in Table 2. We calculate the difference in these features between the generated samples and the real samples as quantitative evaluation indicators, denoted as $\nabla_1$ to $\nabla_8$.

Table 2: Binary geometric features for layout generation evaluation, which is calculated between every two adjacent characters.

| No. | Binary geometric features |
|---|---|
| 1 | Mean vertical distance between geometric centers |
| 2 | Mean horizontal distance between geometric centers |
| 3 | Mean distance between upper bounds |
| 4 | Mean distance between lower bounds |
| 5 | Mean distance between left bounds |
| 6 | Mean distance between right bounds |
| 7 | Mean ratio of heights of bounding boxes |
| 8 | Mean ratio of widths of bounding boxes |

**Readability Assessment.** To assess the structural correctness performance, *AR (Accurate Rate) and CR (Correct Rate)* are two widely used metrics for Chinese string recognition (Su et al., 2009; Wang et al., 2011). We adopt the methods proposed in (Chen et al., 2023) as the text line recognizer, which can get 0.962 AR and 0.958 CR on the test set. We report the recognition metrics of the recognizer on our synthesized text lines, where *higher values indicate more complete and accurate geometric structure*. More details are introduced in Appendix B.2.4.

**Baselines.** 1) In the field of text line recognition, several methods (Peng et al., 2019; Yu et al., 2024) employs synthesized samples to augment the dataset for training. In these synthesized samples, the bounding box (introduced in Section 3.2) of each glyph category is statistically modeled as a Gaussian distribution in the training set. When generating, the bounding box for each character is sampled based on these Gaussian distributions. We denote this layout generation method as *'Gaussian'*. 2) Furthermore, as mentioned before, if no reference samples are provided, our layout generator model can perform unconditional generation, denoted as *'Unconditional'*. We combine the two layout generation methods with our font synthesizer and compare them with our proposed approach *quantitatively and qualitatively*. The default reference text line length is set as 10.

#### 4.3.2 Quantitative Results

As shown in Table 3, we find that: 1) the generated text lines all exhibit AR and CR values exceeding 0.85, demonstrating the complete and correct structures of each character. 2) The layouts generated by the in-context method are closer to real samples in nearly all binary geometric features, which highlights the effectiveness of our proposed layout generative method.

Table 3: Evaluation of Handwritten Text Line Layout Imitation and Readability.

| Baselines | $\nabla_1(\downarrow)$ | $\nabla_2(\downarrow)$ | $\nabla_3(\downarrow)$ | $\nabla_4(\downarrow)$ | $\nabla_5(\downarrow)$ | $\nabla_6(\downarrow)$ | $\nabla_7(\downarrow)$ | $\nabla_8(\downarrow)$ | AR | CR |
|---|---|---|---|---|---|---|---|---|---|---|
| Gaussian | 0.074 | 0.151 | 0.092 | 0.092 | 0.163 | 0.160 | 0.859 | 1.081 | 0.855 | 0.851 |
| Unconditional | 0.048 | 0.132 | 0.034 | 0.063 | 0.160 | 0.139 | 0.366 | 0.408 | 0.856 | 0.852 |
| In-Context | 0.046 | 0.122 | 0.062 | 0.058 | 0.129 | 0.129 | 0.364 | 0.419 | 0.857 | 0.852 |

We further investigate the impact of *varying reference sample lengths* on the performance of layout generator as shown in Figure 6. Intuitively, with increasing length, most metrics tend to improve. Compared to the vertical binary geometric features ($\nabla_1, \nabla_3, \nabla_4, \nabla_7$), the horizontal features ($\nabla_2, \nabla_5, \nabla_6, \nabla_8$) exhibit a larger deviation from real samples, indicating that learning the spacing size is more challenging when imitating the layout style of text lines. Furthermore, with respect to these horizontal features, the disparity between the generated samples and the authentic samples is markedly decreased as the length of the reference sample extends.

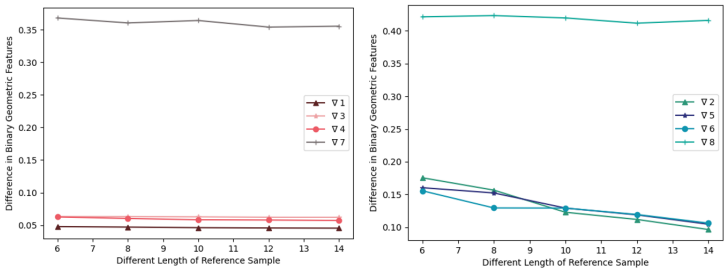


Figure 6: The difference between the mean binary geometric features of generated samples and real samples under different reference sample lengths.

### 4.4 Qualitative Results.

**Layout Case Study.** We specifically select samples with unique layout styles (upward slant) in the test set. Figure 7 shows that although the unconditional layout generation method can produce structurally reasonable layouts, it completely neglects the layout style of the handwritten text line. In comparison, our method *effectively mimics characteristics such as glyph spacing and the slant trend of handwriting*, verifying the necessity of our layout generator.

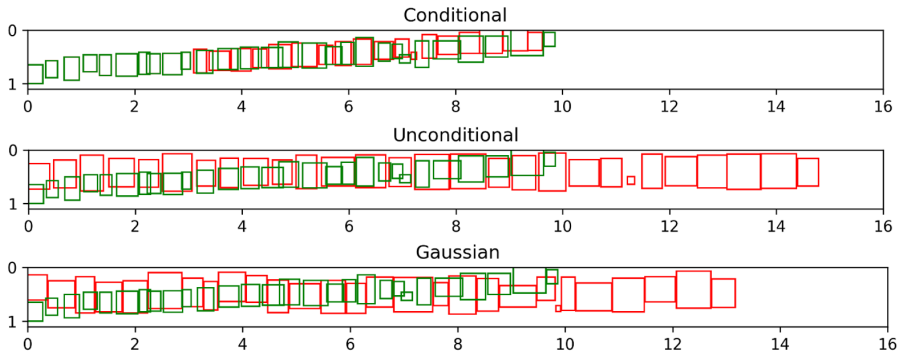


Figure 7: Visualization of character bounding boxes generated by different methods, where green represents the ground truth.

**Subjective Visualization Experiment.** In Figure 8, we select three authors with distinctly different writing styles as imitation targets. We visualized the real samples alongside the generated counterparts. The left columns display the real samples and the right columns display the generated data. It can be observed that our model adeptly imitates the target samples, *capturing both the overall layout style, such as spacing and slant, as well as the calligraphic style of individual characters*.

We take one sample from the real samples and one from the synthesized samples to form a pair, as shown in Figure 9. We create ten similar pairs and ask 20 participants whether the upper and lower lines are written by the same person. More than ninety percent of the responses are 'yes', which demonstrates that it is difficult to distinguish between the real samples and the synthesized ones.

## 5 Conclusions and Limitations

In this paper, we tackle the stylized online handwritten Chinese text line generation task hierarchically, which is almost unexplored. Our model consists of a novel text line layout generator and a stylized diffusion-based character synthesizer. The text line layout generator can arrange glyph positions based on the text contents and writing habits of the given reference samples while the stylized diffusion-based character synthesizer can generate characters with specific categories and calligraphy styles. However, due to the fact that each character is generated independently, our approach encounters difficulties in mimicking styles with extensive cursive connections between characters. An end-to-end text line generation method might be required to address this issue. Furthermore, whether synthesized samples can serve as augmentation data to assist in achieving better results for the recognizer is an open question worth exploring. Last but not least, how to generate more complex handwritten data, such as mathematical formulas based on the hierarchical approach is also an intriguing topic. We consider these as our future work.

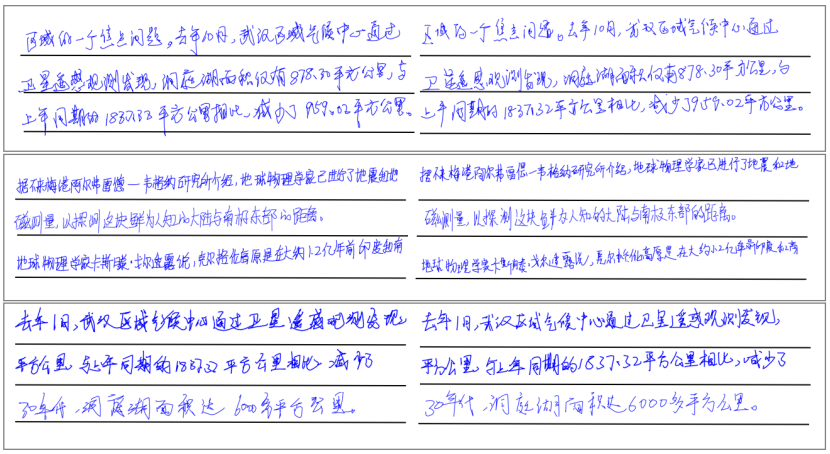

Figure 8: The visualization results. In each block, the left columns display the real samples which are the imitated targets of generated data on the right.

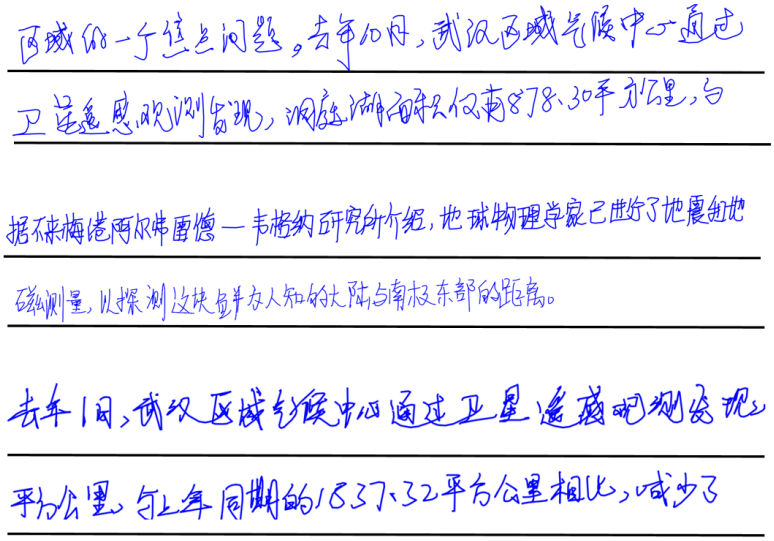

Figure 9: Examples of subjective experiment. Each pair consists of one row from the synthesized samples and the other row from its corresponding target real samples. Participants need to determine whether one pair was written by the same person.

## REFERENCES


Emre Aksan, Fabrizio Pece, and Otmar Hilliges. Deepwriting: Making digital ink editable via deep generative modeling. In *Proceedings of the CHI Conference on Human Factors in Computing Systems*, pp. 1–14, 2018.

Emre Aksan, Thomas Deselaers, Andrea Tagliasacchi, and Otmar Hilliges. CoSE: Compositional stroke embeddings. *Advances in Neural Information Processing Systems*, 33:10041–10052, 2020.

Yi Chen, Heng Zhang, and Cheng-Lin Liu. Improved learning for online handwritten chinese text recognition with convolutional prototype network. In *International Conference on Document Analysis and Recognition*, pp. 38–53. Springer, 2023.

Gang Dai, Yifan Zhang, Qingfeng Wang, Qing Du, Zhuliang Yu, Zhuoman Liu, and Shuangping Huang. Disentangling writer and character styles for handwriting generation. In *Proceedings of the IEEE/CVF Conference on Computer Vision and Pattern Recognition*, pp. 5977–5986, 2023.

Ayan Das, Yongxin Yang, Timothy Hospedales, Tao Xiang, and Yi-Zhe Song. Chirodiff: Modelling chirographic data with diffusion models. *International Conference on Learning Representations*, 2023.

Prafulla Dhariwal and Alexander Nichol. Diffusion models beat gans on image synthesis. *Advances in Neural Information Processing Systems*, 34:8780–8794, 2021.

David H Douglas and Thomas K Peucker. Algorithms for the reduction of the number of points required to represent a digitized line or its caricature. *Cartographica: the international journal for geographic information and geovisualization*, 10(2):112–122, 1973.

Ji Gan and Weiqiang Wang. HiGAN: Handwriting imitation conditioned on arbitrary-length texts and disentangled styles. In *Proceedings of the AAAI Conference on Artificial Intelligence*, volume 35, pp. 7484–7492, 2021.

Yue Gao, Yuan Guo, Zhouhui Lian, Yingmin Tang, and Jianguo Xiao. Artistic glyph image synthesis via one-stage few-shot learning. *ACM Transactions on Graphics*, 38(6):1–12, 2019.

Ian Goodfellow, Jean Pouget-Abadie, Mehdi Mirza, Bing Xu, David Warde-Farley, Sherjil Ozair, Aaron Courville, and Yoshua Bengio. Generative adversarial nets. *Advances in Neural Information Processing Systems*, 27, 2014.

Alex Graves. Generating sequences with recurrent neural networks. *arXiv preprint arXiv:1308.0850*, 2013.

David Ha and Douglas Eck. A neural representation of sketch drawings. In *International Conference on Learning Representations*, 2018.

Jonathan Ho, Ajay Jain, and Pieter Abbeel. Denoising diffusion probabilistic models 2020. *International Conference on Learning Representations*, 2021.

Lei Kang, Pau Riba, Marcal Rusinol, Alicia Fornes, and Mauricio Villegas. Content and style aware generation of text-line images for handwriting recognition. *IEEE Transactions on Pattern Analysis and Machine Intelligence*, 44(12):8846–8860, 2021.

Diederik P Kingma and Max Welling. Auto-encoding variational bayes. In *International Conference on Learning Representations*, 2014.

Yuxin Kong, Canjie Luo, Weihong Ma, Qiyuan Zhu, Shenggao Zhu, Nicholas Yuan, and Lianwen Jin. Look closer to supervise better: one-shot font generation via component-based discriminator. In *Proceedings of the IEEE/CVF Conference on Computer Vision and Pattern Recognition*, pp. 13482–13491, 2022.

Atsunobu Kotani, Stefanie Tellex, and James Tompkin. Generating handwriting via decoupled style descriptors. In *European Conference on Computer Vision*, pp. 764–780. Springer, 2020.

Songxuan Lai, Lianwen Jin, Yecheng Zhu, Zhe Li, and Luojun Lin. Synsig2vec: Forgery-free learning of dynamic signature representations by sigma lognormal-based synthesis and 1d cnn. *IEEE Transactions on Pattern Analysis and Machine Intelligence*, 44(10):6472–6485, 2021.

Zhouhui Lian, Bo Zhao, Xudong Chen, and Jianguo Xiao. Easyfont: a style learning-based system to easily build your large-scale handwriting fonts. *ACM Transactions on Graphics*, 38(1):1–18, 2018.

Jeng-Wei Lin, Chian-Ya Hong, Ray-I Chang, Yu-Chun Wang, Shu-Yu Lin, and Jan-Ming Ho. Complete font generation of chinese characters in personal handwriting style. In *International Performance Computing and Communications Conference*, pp. 1–5. IEEE, 2015.

Cheng-Lin Liu, Fei Yin, Da-Han Wang, and Qiu-Feng Wang. Casia online and offline chinese handwriting databases. In *International Conference on Document Analysis and Recognition*, pp. 37–41. IEEE, 2011.

Wei Liu, Fangyue Liu, Fei Ding, Qian He, and Zili Yi. Xmp-font: self-supervised cross-modality pre-training for few-shot font generation. In *Proceedings of the IEEE/CVF Conference on Computer Vision and Pattern Recognition*, pp. 7905–7914, 2022.

Calvin Luo. Understanding diffusion models: A unified perspective. *arXiv e-prints*, 2022.

Dezhi Peng, Lianwen Jin, Yaqiang Wu, Zhepeng Wang, and Mingxiang Cai. A fast and accurate fully convolutional network for end-to-end handwritten chinese text segmentation and recognition. In *International Conference on Document Analysis and Recognition*, pp. 25–30. IEEE, 2019.

Alec Radford, Luke Metz, and Soumith Chintala. Unsupervised representation learning with deep convolutional generative adversarial networks. *International Conference on Learning Representations*, 2016.

Min-Si Ren, Yan-Ming Zhang, Qiu-Feng Wang, Fei Yin, and Cheng-Lin Liu. Diff-writer: A diffusion model-based stylized online handwritten chinese character generator. In *International Conference on Neural Information Processing*, pp. 86–100. Springer, 2023.

Robin Rombach, Andreas Blattmann, Dominik Lorenz, Patrick Esser, and Bjrn Ommer. High-resolution image synthesis with latent diffusion models. 2021.

Olaf Ronneberger, Philipp Fischer, and Thomas Brox. U-Net: Convolutional networks for biomedical image segmentation. In *International Conference on Medical Image Computing and Computer-Assisted Intervention*, pp. 234–241. Springer, 2015.

Kai Shen, Zeqian Ju, Xu Tan, Yanqing Liu, Yichong Leng, Lei He, Tao Qin, Sheng Zhao, and Jiang Bian. Naturalspeech 2: Latent diffusion models are natural and zero-shot speech and singing synthesizers. *International Conference on Learning Representations*, 2024.

Jascha Sohl-Dickstein, Eric A Weiss, Niru Maheswaranathan, and Surya Ganguli. Deep unsupervised learning using nonequilibrium thermodynamics. *JMLR.org*, 2015.

Jiaming Song, Chenlin Meng, and Stefano Ermon. Denoising diffusion implicit models. *arXiv preprint arXiv:2010.02502*, 2020.

Tong-Hua Su, Tian-Wen Zhang, De-Jun Guan, and Hu-Jie Huang. Off-line recognition of realistic chinese handwriting using segmentation-free strategy. *Pattern Recognition*, 42(1):167–182, 2009.

Shusen Tang and Zhouhui Lian. Write like you: Synthesizing your cursive online chinese handwriting via metric-based meta learning. *Computer Graphics Forum*, 40(2):141–151, 2021.

Shusen Tang, Zeqing Xia, Zhouhui Lian, Yingmin Tang, and Jianguo Xiao. FontRNN: Generating large:cale chinese fonts via recurrent neural network. *Computer Graphics Forum*, 38(7):567–577, 2019.

Ruben Tolosana, Paula Delgado-Santos, Andres Perez-Uribe, Ruben Vera-Rodriguez, Julian Fierrez, and Aythami Morales. Deepwritesyn: On-line handwriting synthesis via deep short-term representations. In *Proceedings of the AAAI Conference on Artificial Intelligence*, volume 35, pp. 600–608, 2021.

Laurens Van der Maaten and Geoffrey Hinton. Visualizing data using t-sne. *Journal of Machine Learning Research*, 9(11), 2008.

Qiu-Feng Wang, Fei Yin, and Cheng-Lin Liu. Handwritten chinese text recognition by integrating multiple contexts. *IEEE transactions on pattern analysis and machine intelligence*, 34(8):1469–1481, 2011.

Canyu Xie, Songxuan Lai, Qianying Liao, and Lianwen Jin. High performance offline handwritten chinese text recognition with a new data preprocessing and augmentation pipeline. In *IAPR International Workshop on Document Analysis Systems*, pp. 45–59. Springer, 2020.

Yangchen Xie, Xinyuan Chen, Li Sun, and Yue Lu. DG-Font: Deformable generative networks for unsupervised font generation. In *Proceedings of the IEEE/CVF Conference on Computer Vision and Pattern Recognition*, pp. 5130–5140, 2021.

Peng Xu, Timothy M Hospedales, Qiyue Yin, Yi-Zhe Song, Tao Xiang, and Liang Wang. Deep learning for free-hand sketch: A survey. *IEEE Transactions on Pattern Analysis and Machine Intelligence*, 45(1):285–312, 2022.

Songhua Xu, Tao Jin, Hao Jiang, and Francis CM Lau. Automatic generation of personal chinese handwriting by capturing the characteristics of personal handwriting. In *Twenty-First IAAI Conference*, 2009.

Zhenhua Yang, Dezhi Peng, Yuxin Kong, Yuyi Zhang, Cong Yao, and Lianwen Jin. Fontdiffuser: One-shot font generation via denoising diffusion with multi-scale content aggregation and style contrastive learning. *Association for the Advancement of Artificial Intelligence*, 2024.

Fei Yin, Qiu-Feng Wang, and Cheng-Lin Liu. Transcript mapping for handwritten chinese documents by integrating character recognition model and geometric context. *Pattern Recognition*, 46 (10):2807–2818, 2013a.

Fei Yin, Qiu-Feng Wang, Xu-Yao Zhang, and Cheng-Lin Liu. ICDAR 2013 chinese handwriting recognition competition. In *International Conference on Document Analysis and Recognition*, pp. 1464–1470. IEEE, 2013b.

Ming-Ming Yu, Heng Zhang, Fei Yin, and Cheng-Lin Liu. An approach for handwritten chinese text recognition unifying character segmentation and recognition. *Pattern Recognition*, pp. 110373, 2024.

Xu-Yao Zhang, Fei Yin, Yan-Ming Zhang, Cheng-Lin Liu, and Yoshua Bengio. Drawing and recognizing chinese characters with recurrent neural network. *IEEE Transactions on Pattern Analysis and Machine Intelligence*, 40(4):849–862, 2017.

Bocheng Zhao, Jianhua Tao, Minghao Yang, Zhengkun Tian, Cunhang Fan, and Ye Bai. Deep imitator: handwriting calligraphy imitation via deep attention networks. *Patteren Recognition*, 2020.

X-D Zhou, J-L Yu, C-L Liu, Takeshi Nagasaki, and Katsumi Marukawa. Online handwritten japanese character string recognition incorporating geometric context. In *International Conference on Document Analysis and Recognition*, volume 1, pp. 48–52. IEEE, 2007.

Jun-Yan Zhu, Taesung Park, Phillip Isola, and Alexei A Efros. Unpaired image-to-image translation using cycle-consistent adversarial networks. In *Proceedings of the IEEE International Conference on Computer Vision*, pp. 2223–2232, 2017.

# A Appendix

# B Appendix

## B.1 Denoising Diffusion Probabilistic Models

In this paper, we adopt the Denoising Diffusion Probabilistic Model (DDPM), which is a generative model that operates by iteratively applying a denoising process to noise-corrupted data. This process, known as the reverse denoising process aims to gradually refine the noisy input towards generating realistic samples. DDPM learns to model the conditional distribution of clean data given noisy inputs, which is derived from the forward diffusion process. Denote the forward process as $q$ and the reverse process as $p$, the forward process starts from the original data $X_0$ and incrementally adds Gaussian noise to the data:

$$q(X_t|X_{t-1}) = \mathcal{N}(X_t; \sqrt{\alpha_t}X_{t-1}, (1-\alpha_t)I) \tag{7}$$

where $\{\alpha_t\}_{t=0}^T$ are noise schedule hyperparameters, $T$ is the total number of timesteps. Due to the Markovian nature of the forward transition kernel $q(X_t|X_{t-1})$, we can directly sample $X_t \sim q(X_t|X_0)$ without reliance on any other $t$:

$$q(X_t|X_0) = \mathcal{N}(X_t; \sqrt{\overline{\alpha}_t}X_0, (1-\overline{\alpha}_t)I), \quad \overline{\alpha}_t = \prod_{i=1}^{t} \alpha_i \tag{8}$$

$$\Rightarrow\ X_t = \sqrt{\overline{\alpha}_t}X_0 + \sqrt{1-\overline{\alpha}_t}\epsilon, \quad \epsilon \sim \mathcal{N}(0, I) \tag{9}$$

The set of $\{\alpha_t\}_{t=0}^T$ and $T$ should guarantee that $\overline{\alpha}_T$ is almost equal to 0, ensuring that the data distribution $q(X_T)$ closely resembles the standard Gaussian distribution. The corresponding normal posterior can be computed as:

$$\begin{aligned} q(X_{t-1}|X_t, X_0) &= \mathcal{N}(X_{t-1}; \mu_q(X_t, X_0), \sigma_q^2(t)I) \\ \mu_q(X_t, X_0) &= \frac{\sqrt{\alpha_t}(1-\overline{\alpha}_{t-1})X_t + \sqrt{\overline{\alpha}_{t-1}}(1-\alpha_t)X_0}{1-\overline{\alpha}_t} \\ \sigma_q^2(t) &= \frac{(1-\alpha_t)(1-\overline{\alpha}_{t-1})}{1-\overline{\alpha}_t} \end{aligned} \tag{10}$$

In training, the denoiser learns to predict the added noise $\epsilon$ in Equation 9 given noisy data $X_t$. The most commonly used objective function is to minimize the deviation between predicted noise and true noise:

$$L(\theta) = E_{t\sim U\{1,T\}, \epsilon\sim N(0,I)}||\epsilon - \epsilon_\theta(X_t(X_0, \epsilon), t)||^2 \tag{11}$$

Theoretically, it is equivariant to optimizing the evidence lower bound of $\log p(X_0)$:

$$L(\theta) \equiv E_{t\sim U\{2,T\}} E_{q(X_t|X_0)} D_{KL}(q(X_{t-1}|X_t, X_0)||p_\theta(X_{t-1}|X_t)) \tag{12}$$

During the reverse process, after substituting Equation 9 into Equation 10 and replacing the true noise $\epsilon$ with the predicted noise $\epsilon_\theta(X_t, t)$, we have:

$$\begin{aligned} p_\theta(X_{t-1}|X_t, t) &= \mathcal{N}(X_{t-1}; \mu_\theta(X_t, t), \sigma_p^2(t)I) \\ \mu_\theta(X_t, t) &= \frac{1}{\alpha_t}X_t - \frac{1-\alpha_t}{\sqrt{1-\overline{\alpha}_t}\sqrt{\alpha_t}}\epsilon_\theta(X_t, t) \\ \sigma_p^2(t) &= \frac{(1-\alpha_t)(1-\overline{\alpha}_{t-1})}{1-\overline{\alpha}_t} \end{aligned} \tag{13}$$

which defines the reverse transition kernel $p_\theta(X_{t-1}|X_t, t)$.

For the hyperparameters of DDPM, we adopt the linear noising schedule proposed by (Ho et al., 2021): $\{T = 1000; \quad \alpha_0 = 1 - 1e^{-4}; \quad \alpha_T = 1 - 2e^{-2}\}$.

## B.2 Implement Details

### B.2.1 Data Preprocessing

We adopt the same configuration as the previous method: we first use the Ramer–Douglas–Peucker algorithm(Douglas & Peucker, 1973) with a parameter of $\epsilon = 2$ to remove redundant points. Then we maintain the aspect ratio and normalize the height of each sample to 1.

### B.2.2 Model Parameterization

For the layout generator model, we adopt a 2-layer LSTM with a hidden size of 128 as the layout generator. *We also attempted to use a transformer as a replacement and found that the results were nearly the same*. Therefore, we chose the simpler and faster LSTM model. For the denoiser model, recall our model consists of a 1D U-Net network as the denoiser, a character embedding dictionary, and a multi-scale calligraphy style encoder. We set the dimension of character embedding as 150 and the dimension of time embedding for diffusion models as 32.

Figure 10 displays the interaction details between 1D U-Net denoiser and style encoder. Each downsampling block, such as $\{f^i, en^i\}_{i=1,2,3}$ consists of three residual dilated convolutional layers and a downsampling layer. The residual dilated convolutional layers have a kernel size of 3 and dilation values of 1, 3, and 5, respectively. The downsampling layer has a stride of 2 and a kernel size of 4. The upsampling blocks of the U-Net are structurally symmetrical to the downsampling block and maintain the same hyperparameters, with the only difference being the substitution of the convolutional layers in the downsampling blocks with deconvolutional layers. Table 4 illustrates the channel numbers of input and output features for each module. Afterward, we employ a simple linear layer to ensure that the output has the same dimensions as the initial data, thus performing the function of noise prediction.

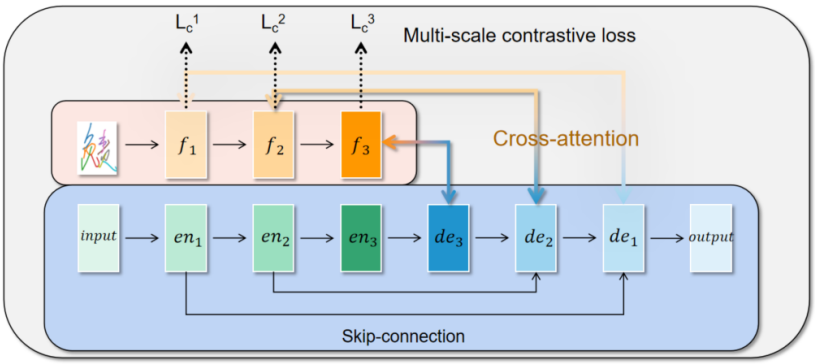


Figure 10: The framework of the multi-scale style encoder and the U-Net Denoiser. The number and stride of downsampling layers of U-Net and the style encoder are aligned, which we set as 3 in this work. The multi-scale style information is injected into U-Net through the cross-attention mechanism.

Table 4: Channel numbers of feature inputs and outputs at different layers..

| | $f^1$ | $f^2$ | $f^3$ | $en^1$ | $en^2$ | $en^3$ | $de^1$ | $de^2$ | $de^3$ |
|---|---|---|---|---|---|---|---|---|---|
| input | 128 | 256 | 512 | 128 | 256 | 512 | 256 | 512 | 1024 |
| output | 256 | 512 | 1024 | 256 | 512 | 1024 | 128 | 256 | 512 |

### B.2.3 Training Details

Actually, the layout planner module and the character synthesizer can be trained jointly. The size information that the layout planner predicts for each character is used as input to the single-character synthesizer, which is expected to generate characters with specific sizes. However, we find that not normalizing the character sizes will affect the model to learn structural information about the characters, leading to unstable generation results. Our approach is to decouple the training process of the layout planner module and the character synthesizer. When training the character synthesizer, we still first normalize all single characters to a fixed height. In this way, the synthesizer only needs to learn to generate characters at a standard size. We take full advantage of the nature that online handwriting data has no background noise, allowing us to directly scale the generated standard-sized characters and fill them into their corresponding bounding boxes.

We implement our model in Pytorch and run experiments on NVIDIA TITAN RTX 24G GPUs. Both training and testing are completed on a single GPU. For training the layout planner, the optimizer is Adam with an initial learning rate of 0.01 and the batch size is 32. For training the diffusion character synthesizer, the initial learning rate is 0.001, the gradient clipping is 1.0, learning rate decay for each batch is 0.9998. We train the whole model with 400K iterations with the batch size of 64, which takes about 4 days.

### B.2.4 Implementation of Evaluation Metrics

**Style Score and Content Score:** For individual character evaluation, due to the limited writing styles represented by individual characters, following previous work(Dai et al., 2023; Tang & Lian, 2021), we combine fifteen characters written by the same author together as input. We train a style classifier with the task of distinguishing 60 writers in the test set, achieving an accuracy of 99.5%. The Style Score refers to the accuracy of classifying generated samples that imitate different styles using this classifier. The higher the style score, the better the model's ability to imitate calligraphy style. Similarly, we utilize all individual character data to train the Chinese character classifier, achieving an accuracy of 98%. Content Score refers to the accuracy of using this classifier to classify the generated samples. The higher the content score, the better the model's ability to generate accurate character structures. Both the style classifier and the content classifier adopt a 1D Convolutional Network, which is the same architecture as the style encoder introduced before.

**Accurate Rate and Correctness Rate:** Unlike single characters, when recognizing text lines, the number of characters within them is unknown. As a result, there may be discrepancies between the total number of characters and the number of correctly recognized characters in the content parsed by the recognizer. Therefore, in the absence of alignment, it is not appropriate to simply use the ratio of correctly recognized characters to the total number of characters as a measure of content score. Instead, evaluation metrics based on edit distance are commonly used:

$$CR = \frac{N_t - D_e - S_e}{N_t} \times 100\% \tag{14}$$

$$AR = \frac{N_t - D_e - S_e - I_e}{N_t} \times 100\% \tag{15}$$

where $N_t$ represents the total number of characters in the real handwritten text line, while $S_e$, $D_e$, and $I_e$ respectively denote substitution errors, deletion errors, and insertion errors.